Synthesis of ZnO Thin Film by Electroplating: Effect of Zinc Concentration on the Structural and Optical Properties

Siregar, Nurdin
Department of Physics, Faculty of Mathematics and Natural Sciences,Universitas Negeri Medan

Motlan and Makmur Sirait
Department of Physics, Faculty of Mathematics and Natural Sciences,Universitas Negeri Medan

https://doi.org/10.5109/6792820

出版情報：Evergreen. 10 (2), pp.715-721, 2023-06. 九州大学グリーンテクノロジー研究教育センター
バージョン：

Synthesis of ZnO Thin Film by Electroplating: Effect of Zinc Concentration on the Structural and Optical Properties

Nurdin Siregar*, Motlan and Makmur Sirait
Department of Physics, Faculty of Mathematics and Natural Sciences,
Universitas Negeri Medan. Jl. Willem Iskandar, Medan Estate, Medan 20221, Indonesia.

*Author to whom correspondence should be addressed:
E-mail: siregarnurdin@unimed.ac.id

(Received January 28, 2023; Revised April 16, 2023; accepted April 20, 2023).

Abstract: ZnO material possesses a huge potential to be utilized as the photoanode in Dye Sensitized Solar Cells (DSSC) application. In this work, we prepared ZnO thin films with different zinc concentrations by a simple and low-cost electroplating technique. XRD analysis reveals that all ZnO thin films with different zinc concentrations have a hexagonal wurtzite crystal structure with crystallite sizes ranging from 19.37 to 32.96 nm. The SEM analysis demonstrated that particle size of the ZnO thin films increased from 46 ±12 to 78±28 nm as the zinc concentration increased from 0.1 to 0.4M. The optical properties analysis revealed the transmittance value of the ZnO thin film for all coating solution concentrations greater than 80%. The band gap energy of the ZnO thin films slightly decrease from 3.20 to 3.16 eV with increasing zinc concentrations from 0.1 to 0.4 M.

Keywords: *ZnO thin film, solution concentration, electroplating method*

1. Introduction

The evolution of solar cell technology from silicon (Si) solar cells to Dye Sensitized Solar Cells (DSSC) continues to increase every year[1]. There is always room for improvement to achieve greater efficiency in the development of DSSC. One of promising approach is the engineering of the semiconductor of the photo-anode. The use of modified ZnO semiconductors as the photoanode electrodes in DSSC is very promising due to the suitable bandgap position of the material, excellent optical, electrical, and piezoelectric properties[2-4].

Various methods for preparing thin film have been explored, including sputtering[5], spray pyrolysis[6], molecular beam epitaxy[7], pulse laser deposition[8], and chemical vapor deposition[9]. However, those methods often have some drawbacks such as high equipment costs and complicated process. Therefore, it is important to develop a simple and low-cost technique for growing ZnO thin film on substrate. Sol-gel spin coating is another relatively low-cost technique approach. Unfortunately, the synthesis process is lengthy and time-consuming, particularly the preparation of the gel[10-11]. To overcome those challenges, the electroplating technique presents to be the best option for growing ZnO thin films. This technique is characterized by its simplicity, cost-effectiveness, and the ability to adjust various parameters to achieve the desired properties. The advantages of the electroplating method include a low temperature process, low cost of the apparatus, the absence of need for vacuum pump to evacuate the chamber, uniform composition, controllable thickness, and excellent microstructural properties[12-13]

There are several reports have utilized electroplating technique to fabricate thin films, showcasing its potential for various applications. For example, Kumar and colleagues prepared aluminum zinc oxide thin films at various deposition potentials for optoelectronic use[14]. Their findings showed that the highest transmittance, reaching 80%, was obtained at a potential of -1.7 V, and the band gap energy decreased with increasing potential. According to report by Navarro-Gázquez and co-workers, the average crystalline size and roughness of the film increased with increasing the electrolyte concentration of $Zn(NO_3)_2$[15]. Sulaiman's group also investigated the effect of the applied potential during the electrodeposition of ZnO and discovered that morphological properties of the resulting thin films were strongly dependent on the applied potential[16]. They found that the surface morphological of the film was a plate-like structure. However, most of those reported works utilized a three-electrode system, including working, counter, and reference electrodes for coating the films[17-19]. This a three-electrode system has several disadvantages such as more complicated set-up and maintenance. In this work, we aim to fabricate ZnO thin films using an electroplating technique with a two-electrode system, which is simpler and easier to set up and maintain than a three-electrode system. The structural and optical properties of the films

with different zinc concentrations will be systematically evaluated.

2. Experimental

2.1 Materials

Zinc foil, indium tin oxide (ITO) glass, and $ZnSO_4$ were purchased from Sigma-Aldrich chemicals company.

2.2 Electroplating

The ITO glass was used as the substrate to grow the ZnO thin film by electroplating technique. Prior to the electroplating procedure, the FTO glass was washed by ultrasonication in acetone and ethanol for each of 5 minutes. A certain amount of $ZnSO_4$ powder was dissolved into 50 mL DI water to obtain a solution concentration with different concentrations such as 0.1, 0.2, 0.3, and 0.4 M. The solution was then stirred for about 15 minutes to let the $ZnSO_4$ homogeneously dispersed. The electroplating was conducted with a two-electrode system with ITO glass (1 x1 cm^2) as working electrode (negative) and zinc foil (1 x1 cm^2) counter electrodes (positive), which were placed parallel to each other with a distance of about 2 cm. All electroplating experiments were carried out with a potentiostat at a constant current density of -10 mA/cm^2 with deposition time of 2.5 minutes. After electroplating, the sample was dried in dry oven at 70 ^{0}C with duration time of 30 min. Then, the sample was annealed at 500 ^{0}C with a heating rate of 10 ^{0}C /min for 2 hours under atmospheric conditions. Lastly, the sample was formed and ready to be used for characterizations.

2.3 Instruments for Characterization

To investigate the structural properties, an X-ray diffractometer (LabX XRD-6100, Shimadzu) was utilized with Cu (λ=1.54Å). The surface morphology and cross section images were captured utilizing a scanning electron microscope (JEOL-6500). A UV-Vis NIR spectrophotometer was used to analyze both transmittance and absorbance spectra. X-ray photoelectron spectroscopy analysis was conducted using a VG ESCA Scientific Theta Probe with Al K_α.

3. Results and discussion

The structural properties of ZnO thin film samples was characterized by an X-ray diffractometer. Figure 1 demonstrates peak diffraction patterns ZnO thin films for various zinc concentrations. The XRD pattern of the ITO substrate was also recorded. As shown in Figure 1, there are several peaks of ITO substrate that located at about 21.45, 30.54, 35.41, 37.64, 41.78, 45.62, 50.95, and 55.90º, which also well agreed with the JCPDS file No. 89-4958 (Indium tin oxide, ITO). As clearly exhibited in Figure 1, all X-ray diffraction patterns of the ZnO thin films at different concentrations show a similar pattern. There are three major additional peaks as compared to the ITO substrate. Those peaks located at about 32, 34.4, and 36.6º for two theta, which correspond to the formation of ZnO with (100), (002), and (101) planes based on the JCPDS file No. 36-1451[20]. All the samples have a hexagonal crystal structure and prefer to grow with an orientation of (101). These results also show that the concentration did not have effect on the crystal growth. To further evaluate the crystal properties of the ZnO thin film, we calculated the full-with half maximum (FWHM). As tabulated in Table 1, the FWHM value increases with increasing the concentration from 0.1 to 0.3M. The ZnO thin film grown with a concentration of 0.3 M had the greatest FWHM value, indicating the lowest crystallinity. Next, the crystallite size of the ZnO thin film was also calculated based on the Scherer formula (eq. 1)[21].

$$D = \frac{0.9\,\lambda}{\beta \cos\theta} \qquad (1)$$

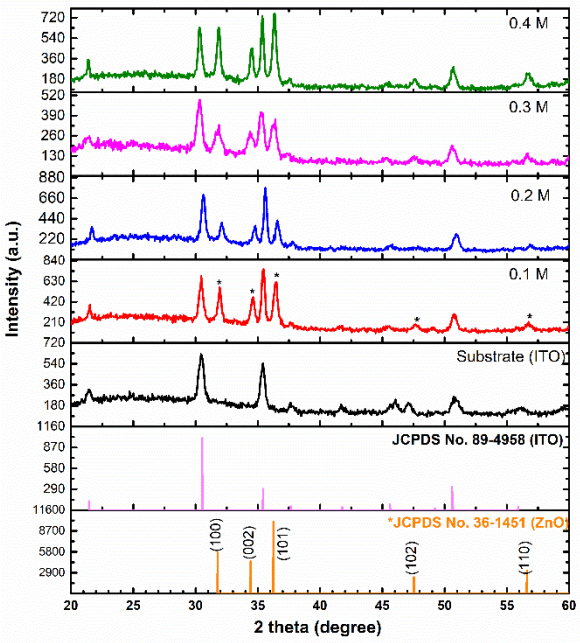

Fig. 1. XRD pattern of ZnO thin films at various concentrations together with substrate and standard JCPDS file.

Table 1. Summary of crystal properties for various zinc concentrations.

M	FWHM	D (nm)	δ x10^{-3} (nm^{-2})	e x 10^{-3}	LP (Å)	
					a	*c*
0.1	0.279	32.96	0.92	4.1	3.23	5.17
0.2	0.326	28.17	1.26	9.4	3.21	5.16
0.3	0.474	19.37	2.67	12	3.24	5.22
0.4	0.309	29.73	1.13	4.1	3.23	5.19

The crystallite sizes of ZnO thin film at concentrations of 0.1, 0.2, 0.3, and 0.4 M were 32.96, 28.17, 19.37, and

29.73 nm, respectively. Again, the ZnO thin film with a concentration of 0.3 M possessed the lowest crystallite size, which confirmed the poorest crystallinity among the as-prepared samples. To further analyze the structural properties of the thin films, the dislocation and density of dislocation were also calculated using eq. 2 and eq. 3, respectively.

$$\delta = \frac{1}{D^2} \quad (2)$$

$$\langle e \rangle = \frac{d - d_o}{d_o} \quad (3)$$

The value of lattice parameters a and c were further computed based on the eqs. 4 and 5[22].

$$a = \frac{\lambda}{\sqrt{3}\sin\theta_{(100)}} \quad (4)$$

$$c = \frac{\lambda}{\sin\theta_{(002)}} \quad (5)$$

Finally, the details crystal properties of ZnO thin film at different zinc concentrations are summarized Table 1.

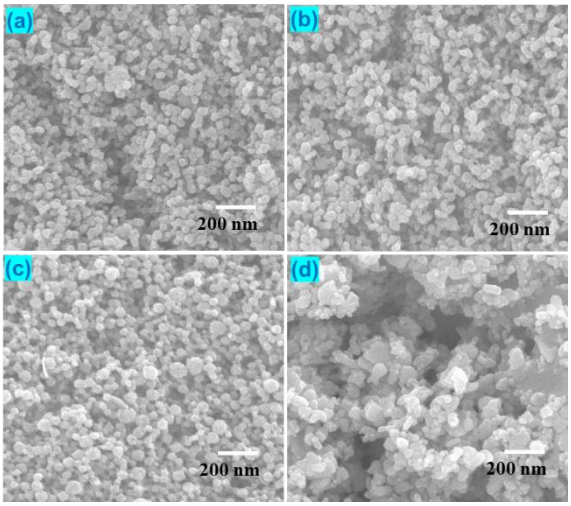

Fig. 2. Electron microscope images of the ZnO Thin Film for various zinc concentration (a) 0.1 M, (b) 0.2 M, (c) 0.3 M, and (d) 0.4 M

The surface morphology of ZnO thin films at various zinc concentrations was observed using a scanning electron microscopy. As revealed in Figure 2, the surface morphological of ZnO thin films consists of a lot of nanoparticles. However, with elevating the concentration of zinc precursor from 0.3 to 0.4 M, the particle size also increases. We then used the image-*J* software to estimate the particle size of nanoparticle on the surface of the films[23]. The average particle sizes were 46±12, 51±12, 58±19, and 78±28 nm for concentrations of 0.1, 0.2, 0.3, and 0.4M, respectively. Figure 3 demonstrates the thickness of the thin films with different zinc concentrations. The actual thickness of ZnO thin films for concentrations of 0.1, 0.2, 0.3, and 0.4M were 1.0, 1.6, 2.2, and 3.2 µm and 1.06, respectively. It is clearly evident that increasing the concentration continuously thickens the thin films.

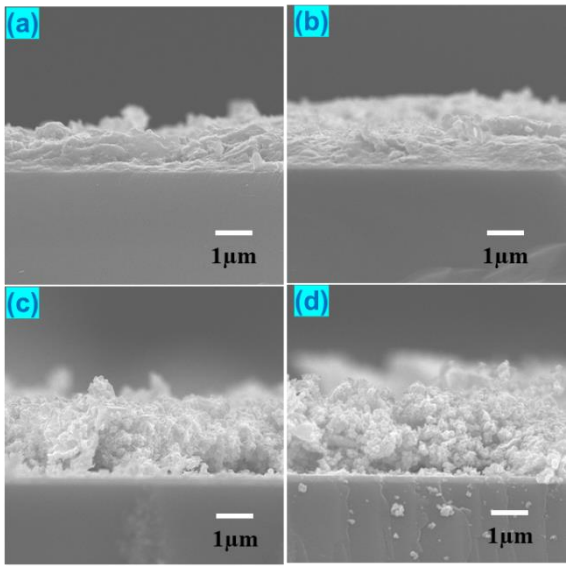

Fig. 3. SEM cross-section images of the ZnO Thin Film at various zinc concentration (a) 0.1 M, (b) 0.2 M, (c) 0.3 M, and (d) 0.4 M

EDS analysis was carried out to determine the elements compositions and the atomic percentages in each sample. It should be noted that to eliminate the other elements contribution from the ITO substrate, the film was stretched off from the substrate and attached to the carbon tape for the EDS analysis. Figure 4 exhibits the EDS spectrum of ZnO thin films with various zinc concentrations. It is clearly seen that Zn and O peaks appear with high intensity for all sample. A weak peak at about 2 keV corresponds to the Pt coating before the SEM test to improve the conductivity, which is common in the field.

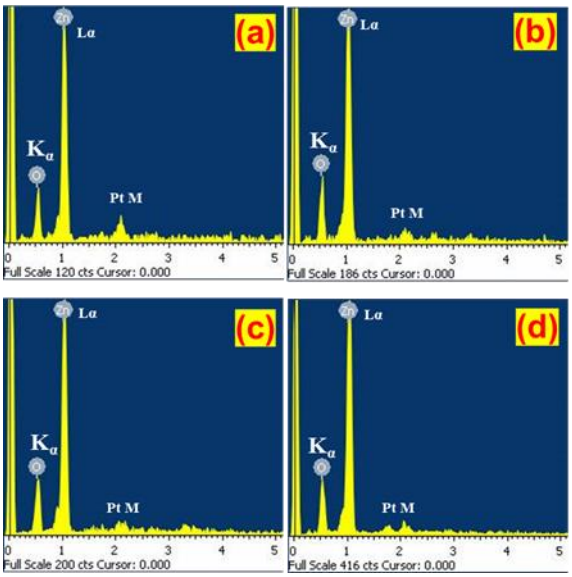

Fig. 4. EDS spectrum of the ZnO thin films at concentrations of (a) 0.1 M, (b) 0.2 M, (c) 0.3 M, and (d) 0.4 M

Based on the peak area of spectrum in Figure 4, the quantitative atomic percentages of Zn and O in each sample can be compouted in Table 2. According to this EDS analysis, the atomic percentage of Zn was about 50% and O was also 50%, which were similar for other concentrations. Therefore, the actual ratio of Zn/O for concentrations of 0.1, 0.2, 0.3 and 0.4M were 1.01, 1.14, 1.00 and 1.06, respectively, which was in line with the theoretical value of 1 (Zn/O=1). The EDS results showed that the concentration of the solution did not significantly affected the atomic percentage of zinc and oxygen. Furthermore, the elemental mapping was performed to evaluate the Zn and O distribution using the representative sample with concentration of 0.2 M. Figure 5b and c clearly exhibits the homogenous distribution of Zn and O on the area mapping (dash line in Figure 5a).

Table 2. Atomic percentage of ZnO thin film at different zinc concentrations

M	Zn (%)	O (%)	Zn/O
0.1	50.23	49.77	1.01
0.2	53.33	46.67	1.14
0.3	50.05	49.95	1.00
0.4	51.39	48.61	1.06

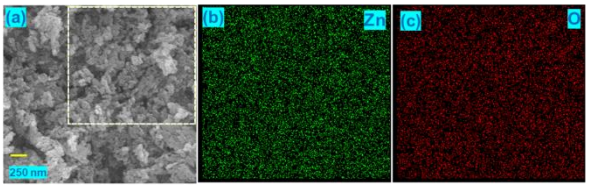

Fig. 5. (a) SEM image for acquiring elemental mapping of (b) Zn and (c) oxygen

To evaluate the surface chemistry of the sample, X-ray photoelectron spectroscopy (XPS) analysis was employed and the result is shown in Figure 6. The high-resolution XPS of Zn 2p in Figure 6a confirms the binding energies of 1020 and 1043 eV, which corresponds to the Zn $2p_{3/2}$ and Zn $2p_{3/2}$, respectively [23]. It also confirms that Zn exist as bivalent (2+) state. Figure 6b demonstrates the high-resolution XPS of O 1s. There are two distinct peaks at 529.6 and 530.2 eV, which related the oxygen in the lattice of ZnO phase and oxygen vacancies, respectively [24]. Based on the peak area and sensitivity factor, the concentrations of zinc and oxygen were 44.77 and 55.23%, respectively, which were similar to EDX results in the previous section.

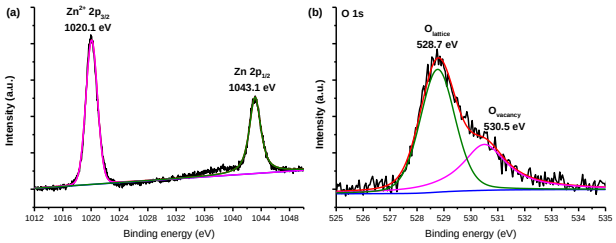

Fig. 6. XPS high-resolution spectrum of (a) Zn 2p and (b) O 1s

Both transmittance and absorbance spectrum of the as-prepared samples were observed and recorded with an UV-Vis spectrophotometer in order to evaluate the optical properties. Figure 7a displays the absorbance of the thin films at the wavelength between 200 to 600 nm. As shown in Figure 7a, all samples exhibit similar spectrum with only different intensity and have strong absorbance values between 300 nm and 400 nm, corresponding to ultraviolet wavelength region. As the concentration of the solution increases, the absorption edge shifts towards shorter wavelengths. Figure 7b depicts the transmittance spectrum of all samples. It can be clearly observed that there is a significant increase in transmittance between approximately 300 and 450 nanometers. By increasing the concentration of the zinc solution in transmittance value decreased while the absorbance increased. This is due to the fact that as the concentration of the solution increases, there are more atoms (thickness of the film increases), and collisions between light particles and atoms become more frequent, making it more difficult for light to pass through. Our finding was also similar to the previous reports[26-28], where the transmittance value decreases with increasing solution concentration. All ZnO thin film samples have transmittance values greater than 80 %, allowing them to be potentially used as the photoanode in DSSCs [29]. To further investigate the optical properties of ZnO thin film, photoluminescence spectroscopy analysis was conducted under an excitation wavelength of 250 nm. The emission was then recorded as wavelength of 300-700 nm. As depicted in Figure 7c, the characteristic emission of all ZnO thin films with different concentrations exhibited a similar emission peak but varying intensities. The highest peak emission located at wavelength of about 400 nm, relating to the UV emission and bandgap of the ZnO. The second peak at 480 nm corresponds to the presence of oxygen vacancy. This presence of oxygen vacancy has been verified by the XPS analysis in the previous section.

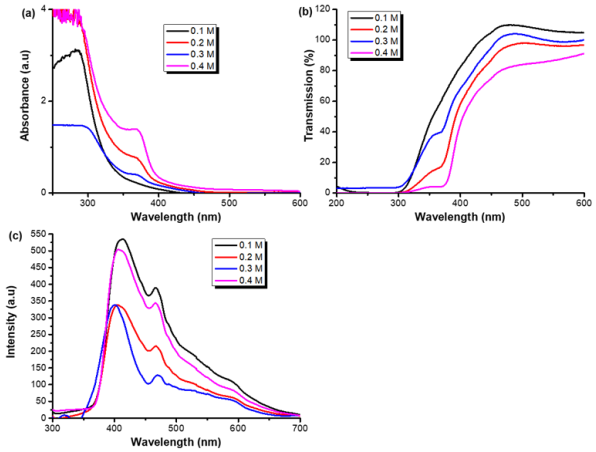

Fig. 7. Optical properties of ZnO thin film (a) absorption, (b) transmission, and (c) photoluminescence spectrum.

The direct band gap value of the samples was further computed to evaluate the effect of zinc concentrations on optical properties of ZnO thin films, according to the relation of absorption and photon energy, which is known as the Tauc plot (Eq. 6)[30].

$$(\alpha hv)^2 = C_D(hv - E_{opt}) \quad (6)$$

Figure 8 demonstrates the Tauc plot to show the bandgap energy of ZnO thin films with variations of concentration. Based on Figure 8, the bandgap values were determined to be 3.20, 3.19, 3.16, and 3.17 eV at zinc concentration of 0.1, 0.2, 0.3, and 0.4 M were, respectively. Clearly, the change in concentration of ZnO thin film solution causes a slight decrease band gap value. This result is in accordance with the previous work[31], which state that the value of bandgap energy drops as the concentration of a solution increases. With excellent structural and optical properties, our ZnO thin film prepared by electroplating technique has a great potential as the photoanode for assembling DSSCs in the next project.

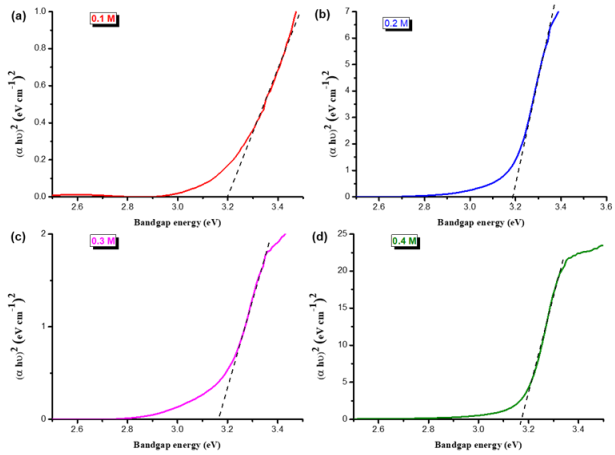

Fig. 8. Tauc Plot of ZnO thin film to determine band gap energy value at different concentrations (a) 0.1 M, (b) 0.2 M, (c) 0.3 M and (d) 0.4 M

4. Conclusion

ZnO thin films with different zinc concentrations have been successfully synthesized by a simple and inexpensive electroplating technique. XRD analysis confirmed that all the ZnO thin film had the hexagonal crystal structure with crystallite size of 19.37 -32.96 nm. The surface the all samples were nano particles with size range of 46 to 78 nm. The solution concentration slightly influences the bandgap energy of ZnO thin films. The transmission value of the film for all concentrations was above 80%. The XPS analysis revealed that our ZnO film consisted of Zn with bivalent, oxygen lattices and vacancies. Our ZnO thin film demonstrate excellent optical and crystallographic properties.

Acknowledgements

This work was supported by Ministry of education, culture, research and technology of Republic of Indonesia under grant number of 021/UN33.8/DRTPM/PL/2022

References

1) Arifin, Zainal, Syamsul Hadi, Bayu Sutanto, and Denny Widhiyanuriyawan. "Investigation of Curcumin and Chlorophyll as Mixed Natural Dyes to Improve the Performance of Dye-Sensitized Solar Cells." *Evergreen*, **9** *(1)* 17–22 (2022) doi.org/10.5109/4774212

2) Saravanakumar, M., Agilan, S. and Muthukumarasamy, N. "Effect of Annealing Temperature on Characterization of ZnO thin films by sol-gel method". *International Journal of Chem Tech Research Coden (USA)*, **6***(5)* 2941-2945 (2014)

3) Siregar, N. and Sirait, M., "Synthesis and optical properties of Sb-doped ZnO thin film by sol-gel spin coating method", *Journal of Physics: Conference Series,* **2193***(1)* 012063 (2022) *DOI* 10.1088/1742-6596/2193/1/012063

4) Shen, H., Shi, X., Wang, Z., Hou, Z., Xu, C., Duan, L., ... & Wu, H. " Defects control and origins of blue and green emissions in sol-gel ZnO thin films. " Vacuum, 202, 11201 (2022) DOI 10.1016/j.vacuum.2022.111201

5) Gupta, Gaurav, R. K. Tyagi, and S. K. Rajput. "A Statistical Analysis of Sputtering Parameters on Superconducting Properties of Niobium Thin Film." *Evergreen*, **8** *(1)* 44–50 (2021) doi.org/10.5109/4372259

6) Kulandaisamy, AJ, JR Reddy, P. Srinivasan, KJ Babu, GK Mani, P. Shankar, and JBB Rayappan. "Room Temperature Ammonia Sensing Properties of ZnO Thin Films Grown by Spray Pyrolysis: Effect of Mg Doping". *Journal of Alloys and Compounds.,* **688** 422–29 (2016) doi.org/10.1016/j.jallcom.2016.07.050

7) Mathew, J. A., Tsiumra, V., Sajkowski, J. M.,

Wierzbicka, A., Jakiela, R., Zhydachevskyy, Y., ... & Kozanecki, A. "Photoluminescence of Europium in ZnO and ZnMgO thin films grown by Molecular Beam Epitaxy." *Journal Luminisence* 251 119167 (2022) doi.org/10.1016/j.jlumin.2022.119167

8) Hussain, A.A., Aadim, K.A. and Slman, H.M. "Structural and optical properties of ZnO doped Mg thin films deposited by pulse laser deposition (PLD)". *Iraqi Journal of Physics*, **12***(25)* 56-61 (2014) doi.org/10.30723/ijp.v12i25.304
9) Narin, P., Kutlu-Narin, E., Kayral, S., Tulek, R., Gokden, S., Teke, A., & Lisesivdin, S. B. "Morphological and optical characterizations of different ZnO nanostructures grown by mist-CVD". *Journal of Luminescence*, *251*, 119158 2022) doi.org/10.1016/j.jlumin.2022.119158
10) Alshammari, A. S., Khan, Z. R., Gandouzi, M., Mohamed, M., Bouzidi, M., Shkir, M., & Alshammari, H. M. "Tailoring the optical properties and the UV detection performance of sol-gel deposited ZnO nanostructured thin films via Cd and Na co-doping". *Optical Materials*, *126*, 112146 (2022). doi.org/10.1016/j.optmat.2022.112146
11) Ţălu, Ş., Boudour, S., Bouchama, I., Astinchap, B., Ghanbaripour, H., Akhtar, M. S., & Zahra, S. "Multifractal analysis of Mg-doped ZnO thin films deposited by sol–gel spin coating method." *Microscopy research and technique*, *85*(4), 1213-1223 (2022) doi.org/10.1002/jemt.23988
12) Khelladi, M., Mentar, L., Beniaiche, A., Makhloufi, L and Azizi, A.. "A study on electrodeposited zinc oxide nanostructures". *J. Mater. Sci.: Mater. Electron*, **24**, 153 (2013) doi.org/10.1007/s10854-012-0973-5
13) Ekanayake, U. M., Dayananda, K. T., Rathuwadu, N., & Mantilaka, M. P. G. " Fabrication of multifunctional smart polyester fabric via electrochemical deposition of ZnO nano-/microhierarchical structures. ." *Journal of Coating Technology* 19(4), 1243-1253. (2022) doi.org/10.1007/s11998-021-00606-6
14) Kumar, K.D.A., Valanarasu, S., Ganesh, V., Shkir, M., AlFaify, S. and Algarni, H. "Effect of potential voltages on key functional properties of transparent AZO thin films prepared by electrochemical deposition method for optoelectronic applications". *Journal of Materials Research*, **33**(11) 1523-1533 (2018) doi:10.1557/jmr.2018.122
15) Navarro-Gázquez, P. J., Blasco-Tamarit, E., Muñoz-Portero, M. J., Solsona, B., Fernández-Domene, R. M., Sánchez-Tovar, R., & García-Antón, J. " Influence of Zn $(NO_3)_2$ concentration during the ZnO electrodeposition on TiO_2 nanosponges used in photoelectrochemical applications." *Ceramic International* 48(10)14460-14472(2022) https://doi.org/10.1016/j.ceramint.2022.01.339
16) Ismail, A.H., Abdullah, A.H. and Sulaiman, Y., 2017. "Physical and electrochemical properties of ZnO films fabricated from highly cathodic electrodeposition potentials." *Superlattices and Microstructures*, **103** 171-179 (2017) doi.org/10.1016/j.spmi.2017.01.028
17) Sun, J., Cao, J., & Jiang, X. "Preparation and photoelectric properties of Bi doped ZnO nanoarrays". *Journal of Alloys and Compounds*, *896*, 162801 (2022) doi.org/10.1016/j.jallcom.2021.162801
18) Ikhioya, I. L., Akpu, N. I., & Ochai-Ejeh, F. U. "Influence of erbium (Er) dopant on the enhanced optical properties of electrochemically deposited zinc oxide (ZnO) films for high-performance photovoltaic systems". *Optik*, *252*, 168486 (2022) doi.org/10.1016/j.ijleo.2021.168486
19) Wang, C., Wang, L. J., Zhang, L., Xi, R., Huang, H., Zhang, S. H., & Pan, G. B. "Electrodeposition of ZnO nanorods onto GaN towards enhanced H2S sensing". *Journal of Alloys and Compounds*, *790*, 363-369 (2019). doi.org/10.1016/j.jallcom.2019.03.084
20) Gultom, N. S., Abdullah, H., and Kuo, D. H. Phase transformation of bimetal zinc nickel oxide to oxysulfide photocatalyst with its exceptional performance to evolve hydrogen. *Applied Catalysis B: Environmental*, **272** 118985 (2020) doi.org/10.1016/j.apcatb.2020.118985
21) Bekele, E.T., Zereffa, E.A., Gultom, N.S., Kuo, D.H., Gonfa, B.A. and Sabir, F.K., "Biotemplated synthesis of titanium oxide nanoparticles in the presence of root extract of Kniphofia schemperi and its application for dye sensitized solar cells. "*International Journal of Photoenergy* **2021** 6648325 (2021) doi.org/10.1155/2021/6648325
22) Himmah Sekar Eka Ayu, Firda Reza Agustiana, Shofirul Sholikhatun Nisa, and Endah Retno Dyartanti. "Synthesis and Characterization of NMC 811 by Oxalate and Hydroxide Coprecipitation Method." *Evergreen*, **9** *(2)*438-442 (2022) doi.org/10.5109/4794169
23) Siregar, N., Panggabean, J.H., Sirait, M., Rajagukguk, J., Gultom, N.S. and Sabir, F.K., "Fabrication of dye-sensitized solar cells (DSSC) using Mg-doped ZnO as photoanode and extract of rose myrtle (*Rhodomyrtus tomentosa*) as natural dye". *International Journal of Photoenergy*, **2021***, 4033692* (2021) doi.org/10.1155/2021/4033692
24) Gultom, N.S., Abdullah, H. and Kuo, D.H.,. "Concept of stagnant capillarity water in the nanoporous SiO_2@(Zn, Ni)(O, S) nanocomposite photocatalyst as a strategy to improve hydrogen evolution." *ACS applied materials & interfaces*, **11**(31) 27760-27769 (2019) doi.org/10.1021/acsami.9b06795
25) Abdullah, H., Gultom, N.S., Hsu, C.C., Shuwanto, H. and Kuo, D.H. "Amorphous-Ni $(OH)_2$ on a Vertically Grown Lamellar Ag-Modified MoS x Thin-Film Electrode with Surface Defects for Hydrogen

Production in Alkaline Solutions." *ACS Applied Energy Materials*, **4**(4) 3869-3880 (2021) doi.org/10.1021/acsaem.1c00252

26) Igweoko, A.E., Augustine, C., Idenyi, N.E., Okorie, B.A. and Anyaegbunam, F.N.C. "Influence of processing conditions on the optical properties of chemically deposited zinc sulphide (ZnS) thin film." *Materials Research Express*, **5**(3) 036413 (2018) doi 10.1088/2053-1591/aab652
27) Abdallah, B., Hussein, R., Al-Kafri, N. and Zetoun, W. "PbS thin films prepared by chemical bath deposition: effects of concentration on the morphology, structure and optical properties. " *Iranian Journal of Science and Technology, Transactions A: Science*, **43**(3) 1371-1380 (2019) doi.org/10.1007/s40995-019-00698-1
28) Andolsi, Y. and Chaabouni, F. "Optoelectronic properties of Cr doped ZnO thin films deposited by RF magnetron sputtering using a powder target." *Journal of Alloys and Compounds*, **818** 152739(2020) doi.org/10.1016/j.jallcom.2019.152739
29) Sathya, M., Claude, A., Govindasamy, P., Sudha, K. and Claude, A. "Growth of pure and doped ZnO thin films for solar cell applications." *Advances in Applied Science Research*, **3**(5)2591-2598 (2012)
30) Abdullah, H., Ko, Y. R., Kuo, D. H., & Gultom, N. S. "Effects of tin in La–Sn-Codoped Zn (O, S) photocatalyst to strongly cleave the Azo bond in Azobenzene with in situ generated hydrogen." *ACS applied materials interfaces* **12**(14) 16186-16199 (2020) doi.org/10.1021/acsami.9b19885
31) Amutha, C., Dhanalakshmi, A., Lawrence, B., Kulathuraan, K., Ramadas, V. and Natarajan, B. Influence of concentration on structural and optical characteristics of nanocrystalline ZnO thin films synthesized by Sol-Gel dip coating method. *Progress in Nanotechnology and Nanomaterials*, **3**(1)13-18 (2014)